Polymer 138 (2018) 218–228

Contents lists available at ScienceDirect

Polymer

journal homepage: www.elsevier.com/locate/polymer

Polymersomes from hybrid peptide-based bottlebrush homopolymers

Sameer Dhawan, M.B. Bijesh, V. Haridas*

Department of Chemistry, Indian Institute of Technology Delhi, New Delhi 110016, India

ARTICLE INFO

Article history:
Received 11 November 2017
Received in revised form
17 January 2018
Accepted 23 January 2018

Keywords:
Polymersomes
Peptide
Homopolymers
Bottlebrush
Norbornene

ABSTRACT

A series of compounds, in which *exo*-norbornene scaffold appended with amino acids, was synthesized. These compounds underwent ring opening metathesis polymerization (ROMP) catalyzed by Grubbs second generation ruthenium catalyst to form polymers with bottlebrush architecture. Four different polymers **P1-P4** were synthesized, differing in number of lipid units and degree of branching. These polymers were well-characterized by ^{1}H NMR and gel permeation chromatographic (GPC) techniques. These peptide-based homopolymers showed an exceptional ability to self-assemble to form polymersomes. The self-assembled structures were characterized by various ultramicroscopic techniques such as scanning electron microscopy (SEM), transmission electron microscopy (TEM) and atomic force microscopy (AFM). The entrapment capability of polymer vesicles was confirmed by dye-encapsulation studies.

1. Introduction

Self-assembly is an elegant strategy for the construction of a wide range of supramolecular architectures such as micelles, ribbons, vesicles, helices, rods, toroids, fibres and tubes [1–4]. Among these, vesicles find immense interest due to their potential applications as drug delivery vehicles, nanoscale reaction vessels and stimuli-responsive materials [5–7]. In the early years, Banghem and Horne reported the spontaneous formation of bilayered vesicular structures from an aqueous dispersion of lecithin and cholesterol molecules [8]. After that many research efforts were directed to design and synthesize molecules for vesicular morphology [9,10]. Presently, there exists a wide range of synthetic systems that display vesicular self-assembly in aqueous and in non-aqueous solvents [11].

Polymersomes are vesicles made up of synthetic amphiphilic copolymers [12,13]. Polymersomes or polymer vesicles contain a hollow interior surrounded by polymeric membrane [14,15]. Hammer and Discher et al. coined this term 'polymersomes' for the vesicles obtained from polyethylene glycol-polyethylethylene (PEG-PEE) diblock copolymer due to their resemblance with liposomes [15]. At present, there exist a large number of synthetic amphiphilic block copolymers that have been reported to form polymersomes with wide range of sizes and surface properties [16,17]. Polymersomes have 10-folds higher membrane strength than those of the liposomes, which imparts better mechanical and chemical stabilities to them [18]. These unique features enabled scientists to explore the potential applications of polymersomes as drug delivery vehicles in order to prevent the premature drug release. Moreover, the hollow interior of polymersomes facilitated the encapsulation of both hydrophilic as well as hydrophobic agents leading to the extension of their applications in the field of drug delivery, diagnostic imaging, DNA-RNA delivery, gene therapy, as artificial organelles, cell mimics, and as nano-reactors for chemical reactions [19–23].

For more than a decade, polymersomes were obtained from the copolymers containing hydrophobic block of various polyesters and polycarbonates, and hydrophilic block of polyethylene glycol (PEG) [24,25]. PEG units were introduced due to their ability to resist plasma protein adsorption which protects them from body's innate immune system [26]. Thus, polymersomes with PEG brushes on their surfaces have stealth character that imparts prolonged blood circulation for targeted drug delivery [27]. Peptide–based polymersomes are more attractive candidates for biomedical applications compared to the conventional synthetic polymers. The reason is not only the presence of metabolizable peptide units but also the unique ability of peptides to form ordered self-assembled structures. Copolymerization of polypeptide blocks with synthetic polymers leads to the formation of ordered nanostructures through intermolecular hydrogen bonding unlike the conventional synthetic copolymers that generally form coil structures [28]. Such

* Corresponding author.
E-mail address: haridasv@iitd.ac.in (V. Haridas).

https://doi.org/10.1016/j.polymer.2018.01.065
0032-3861/

hybrid polymers not only provide the proper control over the assembly but also result in the formation of biologically compatible materials [28]. Many of such hybrid peptidic systems have been reported in the literature along with their biomedical applications [29–31].

Mostly, synthetic polymers that can self-assemble to form polymersomes are copolymers [19–23]. Most of the polymersomes forming polypeptide systems are also diblock or triblock copolymers [26–31]. To our knowledge, synthetic peptide based homopolymers that form polymer vesicles are scarce.

2. Experimental section

2.1. Materials

Amino acids used were of L-configuration and were purchased from SRL India. Reagents were purchased from Sigma-Aldrich or Alfa Aesar. All reagents were used without further purification. Solvents employed in the reactions were distilled/dried prior to use. Progress of reactions was monitored by silica gel thin layer chromatography (TLC). Compounds were purified by silica gel column chromatography. Characterizations were done by the ^{1}H NMR, ^{13}C NMR, IR and High Resolution Mass Spectra (HRMS). IR spectra were recorded on a Nicolet, Protégé 460 spectrometer as KBr pellets. Brucker-DPX-300 spectrometer was used for recording ^{1}H NMR spectra. Tetramethylsilane (TMS) was used as an internal standard. Coupling constants are reported in Hz and the data are reported as s (singlet), d (doublet), br (broad), t (triplet) and m (multiplet), dd (double doublet). High Resolution mass spectra (HRMS) were recorded in Bruker MicrO-TOF-QII model using ESI technique. Melting points were recorded on a Fisher-Scientific melting point apparatus.

2.2. Methods

2.2.1. Scanning electron microscopy (SEM)

Samples were prepared by dissolving 2 mg of polymer per mL of the chosen solvent system. A 10 μL of the sample solution was drop-casted on a fresh glass coverslip. The coverslip was attached to a stub using carbon tape. The sample was dried and coated with ~10 nm of gold. ZEISS EVO Series Scanning Electron Microscope EVO 50 operating at an accelerating voltage of 0.2–30 kV was used for imaging.

2.2.2. Atomic force microscopy (AFM)

About 10 μL of the sample solution was transferred onto freshly cleaved mica and allowed to dry and imaged using AFM. Bruker Dimension Icon atomic force microscope was used for imaging the samples. Tapping mode was used for imaging. Images were recorded at room temperature and data analysis was performed using nanoscope 5.31r software.

2.2.3. High Resolution transmission electron microscopy (HR-TEM)

Sample solutions of polymers were prepared by dissolving 2 mg of polymer per mL of the chosen solvent system. About 5 μL aliquot of the polymer solution was placed on a copper grid (200 mesh) and allowed to dry at room temperature. Samples were viewed using FEI Tecnai G^{2} F20 TWIN transmission electron microscope.

2.2.4. Optical microscopy

Polymer samples were prepared in respective solvent systems. About 10 μL of the polymer solution was mounted on a glass slide and allowed to dry in the open air at room temperature. The sample was viewed using optical microscope (Nikon Eclipse TS100) in bright field.

2.2.5. Fluorescence microscopy

Polymer sample solutions were prepared in chosen solvent systems and were mixed with 0.02 equivalents of 2 mM Rhodamine B dye solution (prepared in the same solvent system). About 10 μL of the sample solution was drop casted on a glass slide and allowed to dry in the open air at room temperature. The unbound Rhodamine B was removed by washing with distilled water. The slide containing the sample was dried by flushing with nitrogen gas and was viewed using optical microscope (Nikon Eclipse TS100) using excitation wavelength $\lambda_{ex} = 510$-560 nm.

2.2.6. Dynamic light scattering (DLS) studies

Polymers were dissolved in chosen solvent systems and the solution was filtered by using Nylon syringe filter (pore size = 0.2 μm). Malvern Zetasizer, NANO ZS90 (Malvern Instruments Limited, U.K.) equipped with a 4 mW He–Ne laser operating at a wavelength of 633 nm was used for measuring the particle size. The scattered light from the sample solution was detected at 90° angle. Measurements were carried out in a glass cell at 25 °C.

2.2.7. Gel permeation chromatography (GPC)

Molecular weight distribution and polydispersity index of the polymers were analyzed by Waters gel permeation chromatography (GPC) equipped with L-2414 refractive index detector and Waters styragel HR3 and HR4 columns in series using THF as eluent (flow rate 1 mL/min; polystyrene standards).

2.2.8. X-ray diffraction studies (XRD)

X-ray crystal structure of monomer was carried out on a BRUKER AXS SMART-APEX diffractometer with a CCD area detector (Mo Kα = 0.71073 Å, monochromator: graphite). The measured intensities were reduced to F2 and corrected for absorption with SADABS. Frames were collected at T = 298 by ω, ϕ and 2θ-rotation at 10 s per frame with SMART. Structure solution, refinement, and data output were carried out with the SHELXTL program. Non-hydrogen atoms were refined anisotropically and C-H hydrogen atoms were placed in geometrically calculated positions by using a riding model.

2.3. Synthesis and characterization

2.3.1. Synthesis of *L1*

To an ice-cooled solution of *tert*-butyloxy carbonyl (Boc) protected alanine **A1** (1.00 g, 5.29 mmol) in dry CH_2Cl_2 (100 mL) was added sequentially, NHS (0.913 g, 7.94 mmol), DCC (1.64 g, 7.94 mmol), hexylamine (0.803 g, 7.94 mmol), NEt_3 (1.11 mL, 7.94 mmol) and left stirred for overnight. The precipitate was filtered off and the filtrate was washed sequentially with 0.2 N H_2SO_4, $NaHCO_3$ and water. The organic layer was collected and dried over anhyd. Na_2SO_4 and evaporated under vacuum to yield 1.20 g of the pure compound. Yield: 83%; Appearance: Yellow viscous liquid; ^{1}H NMR (300 MHz, $CDCl_3$): δ 0.88 (t, J = 6.3 Hz, 3H, C$\underline{H}_3$-), 1.30 (m, 9H, AlaC$\underline{H}_3$- + CH_3(C$\underline{H}_2$)$_3$-), 1.45 (s + m, 11H, -C(C$\underline{H}_3$)$_3$ + -NHCH$_2$C$\underline{H}_2$-), 3.24 (m, 2H, -NHC$\underline{H}_2$-), 4.12 (m, 1H, -NHC$\underline{H}$C=O), 5.06 (br s, 1H, BocN$\underline{H}$-), 6.26 (br s, 1H, -N$\underline{H}$-); ^{13}C NMR (75 MHz, $CDCl_3$): δ 13.95, 18.44, 22.49, 26.47, 28.30, 29.46, 31.43, 39.47, 50.12, 80.01, 155.55, 172.55. IR (KBr): 3302, 3098, 2976, 1716, 1487, 1168, 1062 cm^{-1}. HRMS calcd. for $C_{14}H_{28}N_2O_3Na$, m/z = 295.1992, obtained m/z = 295.1990.

2.3.2. Synthesis of *M1*

To an ice-cooled solution of **L1** (0.200 g, 0.74 mmol) was added HCl in EtOAc (4 mL) and left stirred for 4 h. The reaction mixture was evaporated under vacuum. To the resulting amine was added

NEt_3 (0.400 mL, 2.95 mmol) and dissolved in 50 mL of dry toluene, added *exo*-norbornene dicarboxylic anhydride (0.121 g, 0.74 mmol) and was refluxed overnight. The reaction mixture was evaporated and the residue obtained was chromatographed over silica-gel (100-200 mesh) using EtOAc:Hexane (8:2) as eluent to yield 0.200 g of pure product. Yield: 85%; Appearance: Pale yellow syrup; ^{1}H NMR (300 MHz, $CDCl_3$): δ 0.87 (br t, 3H, C$\underline{H}_3$(CH$_2$)$_3$-), 1.29 (br s, 6H, CH$_3$(C$\underline{H}_2$)$_3$-), 1.4–1.6 (m, 7H, NHCH$_2$C$\underline{H}_2$- + AlaC$\underline{H}_3$ + -CH$_2$NB), 2.70 (s, 2H, -C$\underline{H}$NB), 3.2–3.4 (m, 4H, -C$\underline{H}$NB + -NHC$\underline{H}_2$), 4.73 (q, J = 9 Hz, 1H, -NC$\underline{H}$C=O), 5.9 (br s, 1H, -N$\underline{H}$), 6.30 (s, 2H, -C$\underline{H}$=C$\underline{H}$-); ^{13}C NMR (75 MHz, $CDCl_3$): δ 13.97, 14.55, 22.51, 26.49, 29.37, 31.41, 39.95, 42.87, 45.58, 47.67, 49.83, 138.02, 170.00, 178.01; IR (KBr): 3319, 2928, 2856, 1700, 1644, 1538, 1364, 1199 cm^{-1}; HRMS calcd. for $C_{18}H_{26}N_2O_3Na$, m/z = 341.1841, obtained m/z = 341.1835.

2.3.3. Synthesis of ***P1***

To a solution of **M1** (0.050 g, 0.157 mmol) in dry THF (1 mL) under argon atmosphere, was added Grubbs II generation catalyst (1.33 mg, 0.0018 mmol) and left stirred overnight. Afterwards, the reaction was quenched by adding ethyl vinyl ether. The polymer was precipitated using methanol and the precipitate obtained was dried under vacuum to afford 0.045 g of the product. Yield: Quantitative; Appearance: Colorless film; ^{1}H NMR (300 MHz, $CDCl_3$): δ 0.88 (br t, 3H, C$\underline{H}_3$-), 1.28 (br m, 6H, CH$_3$(C$\underline{H}_2$)$_3$-), 1.40–1.70 (m, 5H, AlaC$\underline{H}_3$ + -NHCH$_2$C$\underline{H}_2$-), 2.80 (br s, 2H, -C$\underline{H}$-), 2.95–3.60 (m, 6H, NHC$\underline{H}_2$ + -C$\underline{H}$), 4.64 (m, 1H, αC$\underline{H}$), 5.49 (br s, 1H, -C$\underline{H}$=C$\underline{H}$-), 5.73 (br s, 1H, -C$\underline{H}$=C$\underline{H}$-), 5.90–6.50 (br s + s, 1H, -N$\underline{H}$-). IR (KBr): 3376, 3080, 2926, 2859, 1702, 1652, 1544, 1379, 1167 cm^{-1}.

2.3.4. Synthesis of ***L2***

To an ice-cooled solution of Boc-aspartic acid **A2** (1.000 g, 3.47 mmol) in dry CH_2Cl_2 (100 mL) was added sequentially, NHS (0.599 g, 5.21 mmol), DCC (1.075 g, 5.21 mmol) hexylamine (0.527 g, 5.21 mmol), NEt_3 (0.73 mL, 5.21 mmol) and stirred overnight. The precipitate was filtered off and the filtrate was washed sequentially with 0.2 N H_2SO_4, $NaHCO_3$ and water. The organic layer was collected and dried over anhyd. Na_2SO_4 and evaporated under vacuum to yield 1.670 g of the crude compound. It was then purified by silica-gel chromatography using EtOAc and hexane as eluent to yield 0.977 g of pure compound. Yield: 71%; Appearance: White solid; Mp: 130–135 °C; ^{1}H NMR (300 MHz, $CDCl_3$): δ 0.89 (br t, J = Hz, 6H, C$\underline{H}_3$-), 1.30 (br m, 12H, CH$_3$(C$\underline{H}_2$)$_3$-), 4.65 (s + m, 9H, -C(C$\underline{H}_3$)$_3$), 1.60 (br m, 4H, NHCH$_2$C$\underline{H}_2$-), 2.40–2.60 (m, 1H, AspC$\underline{H}_2$), 2.80–2.90 (m, 1H, AspC$\underline{H}_2$-), 3.22 (m, 4H, -NHC$\underline{H}_2$-), 4.40 (br s, 1H, -NHC$\underline{H}$C=O), 6.02 (br s, 1H, BocN$\underline{H}$), 6.22 (br s, 1H, -N$\underline{H}$), 6.96 (br s, 1H, -N$\underline{H}$); ^{13}C NMR (75 MHz, $CDCl_3$): δ 13.94, 22.50, 24.95, 25.62, 26.47, 26.56, 28.29, 29.38, 31.44, 33.93, 37.86, 39.62, 49.03, 51.61, 80.04, 155.77, 170.89, 171.24; IR (KBr): 3325, 2929, 2859, 1643, 1532, 1451, 1371, 1309, 1248, 1173, 1044 cm^{-1}.

2.3.5. Synthesis of ***M2***

To an ice-cooled solution of **L2** (1.00 g, 2.42 mmol) was added HCl in EtOAc (5 mL) and left stirred for 4 h. The reaction mixture was evaporated under vacuum and the amine obtained was mixed with NEt_3 (0.40 mL, 2.95 mmol) and dissolved in 50 mL of dry toluene. To this solution, *exo*-norbornene dicarboxylic anhydride (0.397 g, 2.42 mmol) was added and refluxed overnight. The reaction mixture was evaporated and the residue was chromatographed over silica-gel (60-120 mesh) using EtOAc: Hexane (3:7) as eluent to yield 0.70 g of pure product. Yield: 65%; Appearance: Colorless syrup; ^{1}H NMR (300 MHz, $CDCl_3$): δ 0.90 (br t, 6H, C$\underline{H}_3$(CH$_2$)$_3$-), 1.30 (br m, 12H, CH$_3$(C$\underline{H}_2$)$_3$-), 1.50 (br m, 6H, (-NHCH$_2$C$\underline{H}_2$- + -C$\underline{H}_2$NB), 2.74 (m, 4H, Asp C$\underline{H}_2$ + -C$\underline{H}$NB), 3.33 (7H, -NHC$\underline{H}_2$- + C$\underline{H}$NB + -NHC$\underline{H}$C=O), 5.06 (m, 1H, -N$\underline{H}$), 5.84 (br s, 1H, -N$\underline{H}$), 6.31 (s, 2H, -C$\underline{H}$=C$\underline{H}$-NB); ^{13}CNMR (75 MHz, $CDCl_3$): δ 13.95, 22.50, 26.51, 26.54, 29.27, 29.37, 29.64, 31.40, 31.42, 33.89, 36.21, 39.87, 43.04, 45.52, 47.71, 47.86, 50.56, 137.99, 170.52, 177.60; IR (KBr): 3352, 2927, 2860, 1771, 1703, 1547, 1455, 1383, 1185 cm^{-1}. HRMS calcd. for $C_{25}H_{39}N_3O_4Na$, m/z = 468.2838, obtained 468.2849.

2.3.6. Synthesis of ***P2***

Compound **M2** (0.05 g, 0.112 mmol) was dissolved in dry THF (0.5 mL) added Grubbs IInd Generation catalyst (1.00 mg, 0.001 mmol) under argon atmosphere,and left stirred for overnight. The reaction was quenched by addition of ethyl vinyl ether. The polymer was precipitated using methanol and the precipitate was dried under vacuum to yield 0.045 g of the product. Yield: Quantitative; Appearance: Light brown solid; ^{1}H NMR (300 MHz, $CDCl_3$): δ 0.88 (br t, 6H, C$\underline{H}_3$-), 1.20 (br m, 12H, CH$_3$(C$\underline{H}_2$)$_3$-), 1.47 (br m, 4H, -NHCH$_2$C$\underline{H}_2$-), 1.60 (br s, 2H, NB-C$\underline{H}_2$), 2.50–3.90 (br m, 8H, -NHC$\underline{H}_2$ + -C$\underline{H}$-), 4.95 (br s, 1H, $\alpha\underline{H}$), 5.45 (br s, 1H, -C$\underline{H}$=C$\underline{H}$-), 5.68 (br s, 1H, -C$\underline{H}$=C$\underline{H}$-), 6.18 (br s, 1H, -N$\underline{H}$-), 6.90 (br s, 1H, -N$\underline{H}$-). IR (KBr): 3368, 2937, 2856, 1706, 1644, 1550, 1388, 1175, 1062 cm^{-1}.

2.3.7. Synthesis of ***M3***

To aspartic acid methyl ester **A3** (0.24 g, 1.22 mmol) in dry toluene (50 mL), was added NEt_3 (0.34 g, 2.44 mmol), followed by *exo*-norbornene dicarboxylic anhydride (0.20 g, 1.22 mmol) and refluxed overnight. The reaction mixture was evaporated and the residue was purified by silica gel chromatography (60-120 mesh) using EtOAc:Hexane (2:8) as eluent to obtain 0.285 g of pure product. Yield: 76%; Appearance: White solid; Mp: 114–116 °C; ^{1}H NMR (300 MHz, $CDCl_3$): δ 1.53 (br q, 2H, -C$\underline{H}_2$NB), 2.73 (q, J = 3.9 Hz, 2H, -C$\underline{H}$NB), 2.99 (m, 1H, -C$\underline{H}$NB), 3.23–3.35 (m, 3H, -C$\underline{H}$NB + AspCH$_2$-), 3.69 (s, 3H, -OC$\underline{H}_3$), 3.73 (s, 3H, -OC$\underline{H}_3$), 5.19 (m, 1H, -NC$\underline{H}$C=O), 6.31 (s, 2H, -C$\underline{H}$=C$\underline{H}$-NB); ^{13}C NMR (75 MHz, $CDCl_3$): δ 33.01, 42.68, 45.44, 45.61, 47.65, 47.85, 48.68, 52.04, 52.98, 138.04, 168.19, 170.35, 176.93; IR (KBr): 3464, 2959, 2359, 1710, 1383, 1184, 1004 cm^{-1}; HRMS calcd. for $C_{15}H_{17}NO_6Na$, m/z = 330.0954, obtained m/z = 330.0956.

2.3.8. Synthesis of ***P3***

To a solution of **M3** (0.061 g, 0.197 mmol) in dry THF (0.5 mL) was added Grubbs IInd generation catalyst (1.4 mg, 0.0017 mmol) under argon atmosphere and stirred overnight. The reaction was quenched by the addition of ethyl vinyl ether. The polymer was precipitated using methanol and the precipitate obtained was dried under vacuum to yield 0.060 g of the product. Yield: Quantitative; Appearance: Colorless film; ^{1}H NMR (300 MHz, $CDCl_3$): δ 1.50 (br, 2H, -C$\underline{H}_2$), 2.65–3.4 (m, 6H, AspC$\underline{H}_2$ + -C$\underline{H}$), 3.49 (s, 3H, -OC$\underline{H}_3$), 3.6–3.8 (s + s, 3H, -OC$\underline{H}_3$), 5.12 (br s, 1H, αC$\underline{H}$), 5.51 (br s, 1H, -C$\underline{H}$=C$\underline{H}$-), 5.74 (br s, 1H, -C$\underline{H}$=C$\underline{H}$-); IR (KBr): 3370, 2926, 2861, 1701, 1554, 1384, 1073 cm^{-1}.

2.3.9. Synthesis of ***A4***

To an ice-cooled solution of **A2** (1.000 g, 4.29 mmol) in dry CH_2Cl_2 was added sequentially, NHS (0.987 g, 8.58 mmol), DCC (1.769 g, 8.58 mmol), **A3** (1.696 g, 8.58 mmol), NEt_3 (1.19 mL, 8.58 mmol) and left to stir overnight. The precipitate was filtered off and the filtrate was washed sequentially with 0.2 N H_2SO_4, $NaHCO_3$ and water. The organic layer was collected and dried over anhyd. Na_2SO_4 and evaporated under vacuum to obtain 2.70 g of the crude compound. It was then chromatographed using silica gel using EtOAc and hexane as eluent to obtain 1.23 g of pure compound. Yield: 55%; Appearance: White solid; Mp: 91–95 °C; ^{1}H NMR (300 MHz, $CDCl_3$): δ 1.48 (s, 9H, -C(C$\underline{H}_3$)$_3$), 2.60–3.10 (m, 6H, AspC$\underline{H}_2$-), 3.70 (s, 6H, -OC$\underline{H}_3$), 3.80 (s, 6H, -OC$\underline{H}_3$), 4.53 (br s, 1H, $\alpha\underline{H}$), 4.85 (m, 2H, $\alpha\underline{H}$), 6.01 (br d, 1H, BocN$\underline{H}$), 6.78 (d, J = 8.4 Hz, 1H, -N$\underline{H}$), 7.58 (d, J = 7.2 Hz, 1H, -N$\underline{H}$); ^{13}C NMR (75 MHz, $CDCl_3$): δ 24.00,

27.21, 34.88, 36.30, 47.54, 47.70, 50.09, 51.00, 51.05, 51.75, 51.78, 79.28, 154.57, 169.65, 169.84, 169.97, 170.06, 170.23, 170.39; IR (KBr): 3331, 2953, 1745, 1652, 1531, 1437, 1369, 1290, 1169, 1053 cm^{-1}; HRMS calcd for $C_{21}H_{33}N_3O_{12}K$, m/z = 558.1701, obtained m/z = 558.1673.

*2.3.10. Synthesis of **M4***

To an ice-cooled solution of **A4** (0.298 g, 0.574 mmol) in EtOAc, added HCl in EtOAc and left stirred for 4 h. The reaction mixture was evaporated under vacuum, the resulting amine was dissolved in 50 mL of dry toluene and mixed with NEt_3. To this solution was added *exo*-norbornene dicarboxylic anhydride (0.094 g, 0.573 mmol) and refluxed overnight. The reaction mixture was evaporated and the residue was chromatographed over silica gel (60-120 mesh) using EtOAc:Hexane as eluents to yield 0.075 g of pure product. Yield: 23%; Appearance: Colorless syrup; ^{1}H NMR (300 MHz, $CDCl_3$): δ 1.51 (d, J = 10.2 Hz, 1H, -CH_2NB), 1.65 (br, 1H, -CH_2NB), 2.65–3.10 (s + m, 8H, AspCH_2- + -CHNB), 3.25–3.45 (m, 2H, -CHNB), 3.65–3.80 (m, 12H, -OCH_3), 4.84 (br m, 2H, α CH), 5.14 (m, 1H, α CH), 6.29 (s, 2H, -CH=CH,NB), 6.80 (d, J = 7.8 Hz, 1H, -NH-), 7.64 (d, J = 8.4 Hz, 1H, NH-); ^{13}C NMR (75 MHz, $CDCl_3$): δ 35.63, 35.80, 35.97, 43.13, 45.51, 45.55, 47.78, 48.57, 47.88, 48.91, 50.25, 52.06, 52.84, 52.92, 138.09, 167.27, 169.87, 170.75, 171.14, 171.23, 177.38, 177.62; IR (KBr): 3527, 3421, 3327, 2937, 1703, 1524, 1441, 1375, 1218 cm^{-1}; HRMS calcd. for $C_{25}H_{31}N_3O_{12}Na$, m/z = 588.1805, obtained m/z = 588.1801.

*2.3.11. Synthesis of **P4***

Compound **M4** (0.05 g, 0.088 mmol) was dissolved in dry THF (0.5 mL) and added Grubbs IInd generation catalyst (0.80 mg, 0.0009 mmol) under argon atmosphere and left to stir overnight. Afterwards, the reaction was quenched by addition of ethyl vinyl ether (3 mL), the polymer was precipitated using methanol and the precipitate was dried under vacuum to yield 0.045 g of the product. Yield: Quantitative; Appearance: Brown semi-solid; ^{1}H NMR (300 MHz, $CDCl_3$): δ 1.10–1.30 (br s + s, 2H, -CH_2), 2.70–3.50 (br m, 8H, CH + AspCH_2-), 3.60–3.80 (m, 12H, -OCH_3), 4.81 (br s, 3H, αCH-), 5.03 (br s, 1H, -CH=CH-), 5.45 (br s, 1H, -CH=CH-), 5.72 (br s, 2H, -NH-); IR (KBr): 3359, 2943, 2835, 2647, 2527, 1737, 1541, 1439, 1386, 1283, 1227, 1116, 1027 cm^{-1}.

*2.3.12. Synthesis of **M5***

To an ice-cooled solution of **A3** (0.24 g, 1.22 mmol) in dry toluene (50 mL) was added NEt_3 (0.34 mL, 2.44 mmol), followed by *endo*-norbornene dicarboxylic anhydride (0.20 g, 1.22 mmol) and refluxed overnight. The reaction mixture was evaporated and the residue was chromatographed using silica gel (100-200 mesh) using EtOAc:Hexane (2:8) as eluent to yield 0.337 g of pure product. Yield: 90%; Appearance: White solid; Melting point: 88-90 °C; ^{1}H NMR (300 MHz, $CDCl_3$): δ 1.54 (d, J = 8.4 Hz, 1H, -CH_2NB), 1.74 (d, J = 7.5 Hz, 1H, -CH_2NB), 2.69–2.83 (m, 1H, -CHNB), 3.15–3.25 (m, 1H, -CHNB), 3.31 (m, 2H, AspCH_2-), 3.41 (s, 2H, -CHNB), 3.75 (s, 6H, -OCH_3), 5.13 (t, J = 6.0 Hz, 1H, -NCHC=O), 6.07 (s, 2H, -CH=CH-); ^{13}C NMR (75 MHz, $CDCl_3$): δ 33.31, 45.05, 45.21, 45.71, 45.82, 48.31, 51.96, 52.18, 52.58, 134.15, 168.15, 170.22, 176.13; IR (KBr): 3463, 2955, 1745, 1441, 1383, 1181, 1005 cm^{-1}. HRMS calcd. for $C_{15}H_{17}NO_6Na$, m/z = 330.0954, obtained m/z = 330.0939.

3. Results and discussion

Bioactivity of a polymer is largely dependent on the factors such as molecular weights, polydispersities and backbone configuration [32]. Therefore, in order to achieve the high bioactivity, peptidic homopolymers must be synthesized with high degree of control over afore mentioned factors. Ring opening metathesis polymerization (ROMP) of norbornene derivatives is a convenient route to synthesize polymers with controlled polydispersities and tacticities [33,34]. Moreover, monomers of ROMP are easy to synthesize and can be fine-tuned for achieving myriad of polymer 3D configurations, hence ROMP is highly attractive strategy for fabricating novel polymeric materials [35–41]. Additionally, ROMP is well-compatible with the amino acid-derived norbornene derivatives [42,43].

Based on this notion, we designed and synthesized various norbornene amino acid conjugates as monomers for ROMP. The monomers were designed in such a way so that after polymerization, bottlebrush architectures are obtained. Bottlebrush polymers are the graft polymers containing long side chains attached to a polymeric backbone. The steric repulsion between the pendent side chains causes the extension of the polymeric backbone leading to the formation of bottlebrush-like architectures. Such architectures can self-assemble to form a variety of nanostructures such as nanowires, nanotubes, nanocapsules, and nanocylinders [44–47]. This served as an inspiration for the design and synthesis of self-assembling hybrid peptidic bottlebrush polymers.

Four different types of monomers **M1-M4** (Scheme 1) were designed with varying number of lipid units and degree of branching. It is well-known that *exo*-norbornene derivatives are suitable candidates for ROMP [48–50], therefore, we designed and synthesized all the monomers **M1-M4** based on *exo*-norbornene scaffold. The monomer **M1** based on alanine amino acid contains one lipid chain. The N-protected alanine **A1** was coupled with hexylamine in the presence of dicylcohexylcarbodiimide (DCC) and *N*-hydroxysuccinimide (NHS) to give **L1**. Deprotection with EtOAc/HCl and subsequent reaction with *exo*-norbornene dicarboxylic anhydride in the presence of triethylamine (NEt_3) yielded the monomer **M1** in 85% yield (Scheme 1).

Further, the Boc protected aspartic acid **A2** was coupled with hexylamine in the presence of DCC and NHS to obtain **L2**. Deprotection and subsequent reaction with *exo*-norbornene dicarboxylic anhydride resulted in the formation of monomer **M2** (65% yield) structurally similar to **M1** with higher number of lipid units.

Monomer **M3** without lipid unit was synthesized as a control compound. For this, aspartic acid dimethyl ester **A3** was treated with *exo*-norbornene dicarboxylic anhydride in the presence of NEt_3 to afford monomer **M3** in 76% yield.

Further branching was introduced in the monomer design to investigate its effect on self-assembly. For this, Boc protected aspartic acid **A2** was coupled with aspartic acid methyl ester **A3** in the presence of DCC and NHS to obtain first generation Asp-based dendron **A4**, which after Boc deprotection and successive reaction with *exo*-norbornene dicarboxylic anhydride yielded monomer **M4** with increased degree of branching as compared to **M3**.

All the monomers **M1-M4** were, then, subjected to ROMP using Grubbs second generation ruthenium catalyst **G2** (SIMes) $(PCy_3)(Cl)_2Ru$ = CHPh (where SIMes: 1,3-dimesityl-4,5-dihydroimidazol-2-ylidene and Cy: cyclohexyl); under an argon atmosphere to afford the corresponding polymers **P1-P4** (Scheme 2) in quantitative yields. The formation of polymer was confirmed by comparing the ^{1}H NMR of the monomer and the corresponding polymer. The disappearance of olefinic protons (-CH=CH-, appeared as singlet at δ = 6.30 ppm) of **M1** (marked by a black and red arrow in Fig. 1A-B) upon polymerization and the appearance of a new set of peaks around δ = 5.5–6.0 ppm (marked by a blue arrow in Fig. 1B) supported the formation of polymer **P1** [49,51].

The molecular weight distribution of the polymers was determined by gel permeation chromatography (GPC) using THF as eluent. The average molecular weight of polymers **P1-P3** was found to lie in the range of 7000–25000 Daltons (Da) having polydispersity index (PDI) 1.38–1.56 (Figures S1-S3). Polymer **P3** with

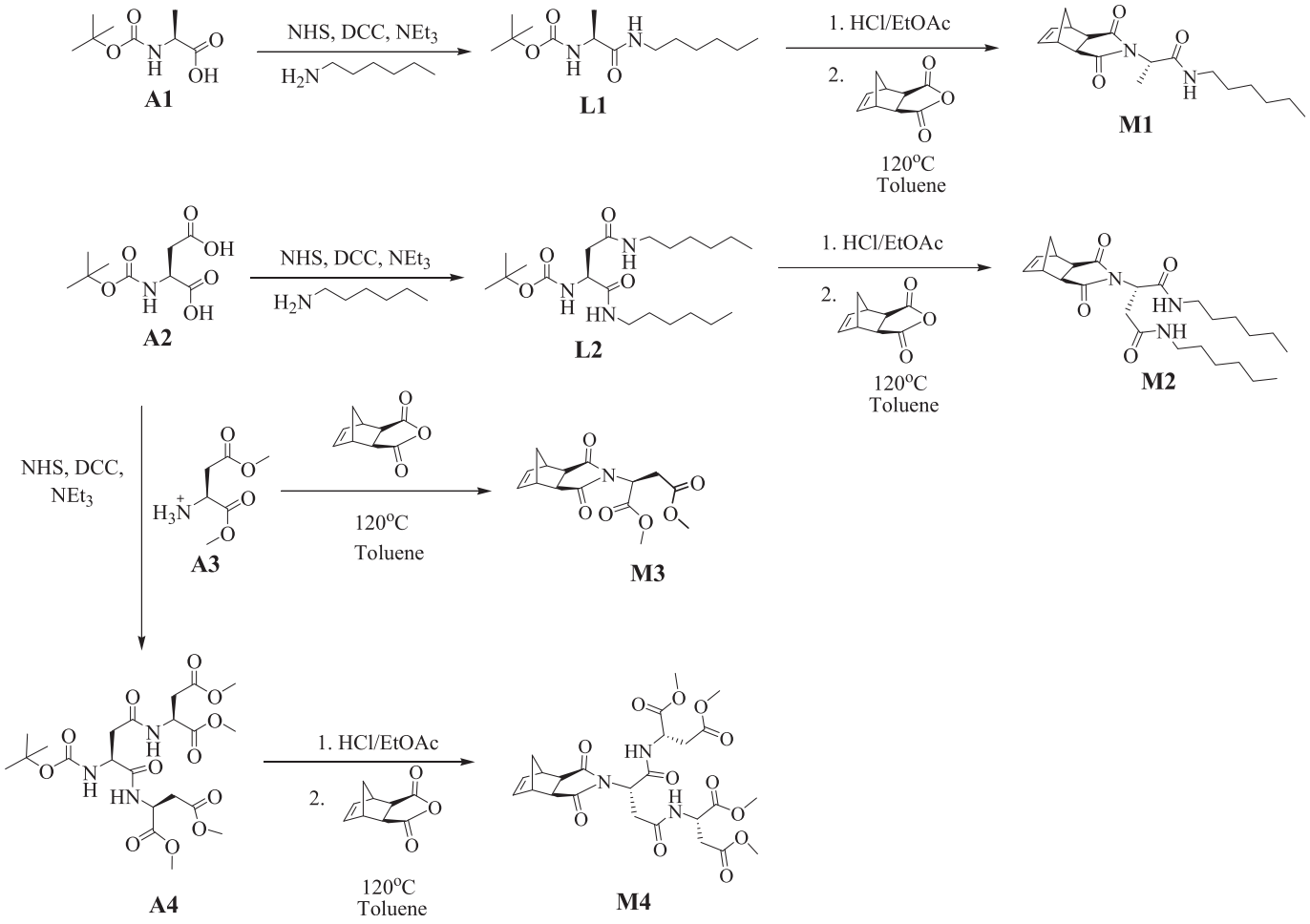

Scheme 1. Synthesis of *exo*-norbornene cored amino acid based monomers **M1-M4**.

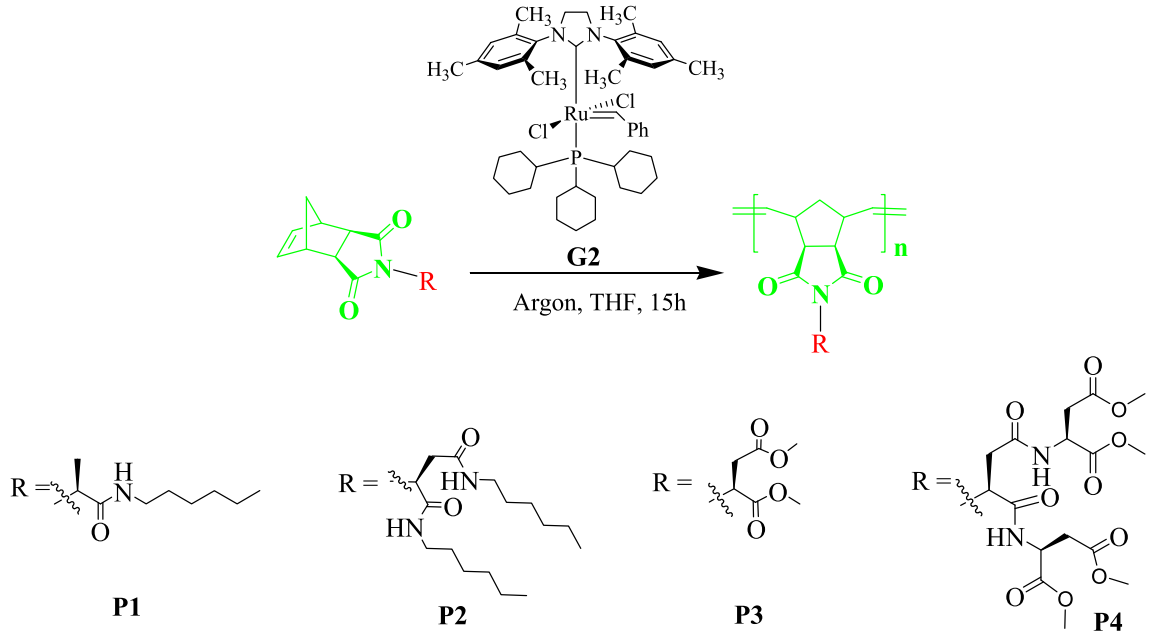

Scheme 2. Synthesis of polymers by ROMP in the presence of Grubbs second generation catalyst.

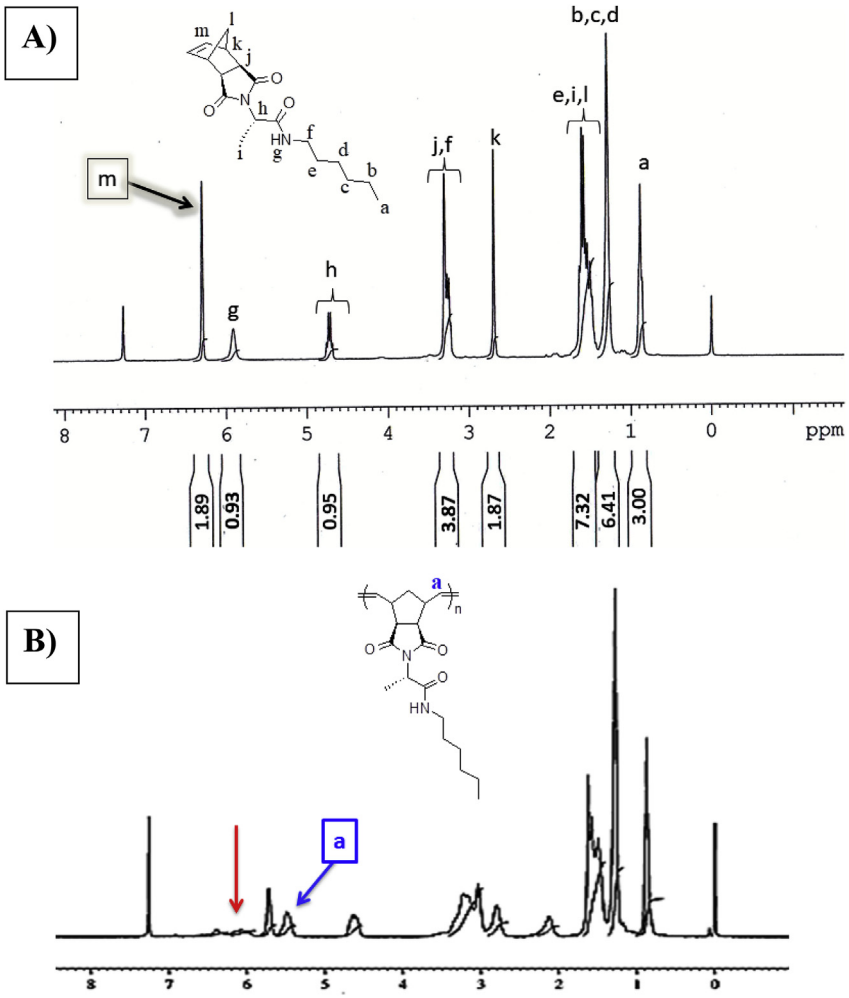

Fig. 1. Comparison between ^{1}H NMR spectra of A) monomer **M1** in $CDCl_3$, B) bottlebrush polymer **P1** in $CDCl_3$.

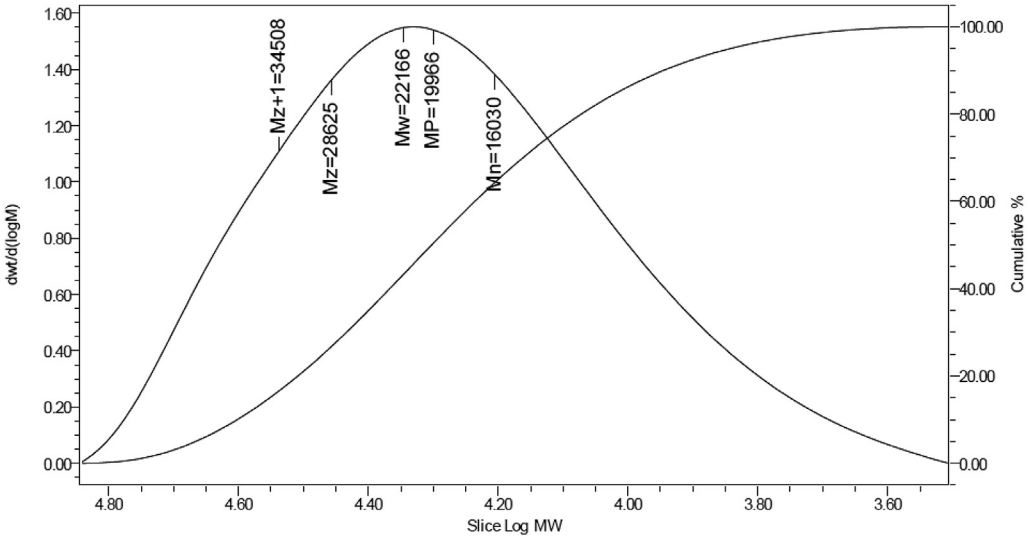

Fig. 2. Molecular weight distribution curve for polymer **P3** as obtained by GPC analysis.

least degree of lipidation and branching showed the highest average molecular weight of 22,166 Da with PDI of 1.38 (Fig. 2, S3).

Polymer **P1** with one pendent lipid arm showed an intermediate value of average molecular weight, while **P2** with two pendent lipid arms showed the least value of average molecular weight. Polymer **P4** was found to be insoluble in THF and hence, its molecular weight was not determined.

All the monomers **M1-M4**, upon polymerization, formed the bottlebrush-like architectures as depicted in Fig. 3 [52–54]. We envisaged that bottlebrush-like polymeric architectures carrying chiral amino acids will direct the self-assembly leading to the formation of interesting morphologies. Therefore, we analyzed the self-assembling behavior of polymer **P1** in chloroform:methanol (1:2). Atomic force microscopic (AFM) measurements revealed the formation of polymer vesicles of diameter ~100-400 nm with a height of around 20 nm (Fig. 4a). The scanning electron microscopy (SEM) and optical microscopy also confirmed the formation of vesicular morphology (Fig. 4c, S4). The size distribution from the dynamic light scattering (DLS) measurements showed the average diameter of vesicles as 459 nm (Figure S5a). Further, the TEM also revealed the formation of vesicles (Fig. 4e, S4). Interestingly, the thickness of the vesicle membrane is not visible from TEM images, implying that the vesicles are soft in nature [55].

In order to investigate the effect of increased number of lipid units, our next attempt was to explore the self-assembly of polymer **P2** with two lipid arms. Therefore, we performed the SEM on **P2** dissolved in chloroform: methanol 1:1. Interestingly, SEM revealed the vesicular morphology with a broad size distribution (Fig. 5a, S6). TEM also confirmed the formation of soft vesicles (Fig. 5b, S6). DLS measurements showed the average size of vesicles around 531 nm (Figure S5b). This demonstrated that the presence of more number of lipid chains in the polymeric framework did not alter the vesicular morphology.

Further, the AFM imaging of polymer **P3** with least degree of lipidation also revealed the spherical vesicular morphology with diameter ranging from 200-400 nm (Fig. 4b). The average height of vesicles was found to be ~50 nm. The SEM and TEM analysis also endorsed the vesicle formation in chloroform: methanol (Fig. 4d and f, S7). The DLS analysis showed that size of vesicles lie in the range of 300–500 nm (Figure S5c), which is consistent with the AFM measurements.

In order to understand the effect of branching on the self-assembly, we studied the self-assembly of aspartic acid-based polymer **P4**. Interestingly, the polymer **P4** with least degree of lipidation and highest degree of branching self-assembled to form polymer vesicles in chloroform: methanol (1:1) as demonstrated by SEM, TEM and AFM microscopic analysis (Fig. 6a-c, S8). The cross sectional analysis of vesicles revealed the range of diameter ~200-400 nm and height ~40 nm (Fig. 6a). DLS also confirmed the size of vesicle as 200-300 nm (Figure S5d).

Further, to explore the entrapment capacity of these polymersomes, we performed the dye-encapsulation experiments using fluorescent dye Rhodamine B. The polymer solution was mixed with Rhodamine B dye and deposited on a glass slide, dried, and washed with water to remove the unbound dye. The fluorescence microscopic analysis revealed the successful encapsulation of Rhodamine B as indicated by red spheres in all the polymers **P1-P4** (Figs. 5-6, S4, S6-S8). This demonstrated the utility of the polymersomes to act as potential encapsulating agents.

In all the polymers **P1-P4**, the variations are on the pendent arms, while the polymeric backbone is made from *exo*-norbornene units. We further synthesized *endo*-cis norbornene-cored simplest monomer **M5** (Scheme 3) to see the effect of stereochemistry on self-assembly. For this, aspartic acid methyl ester **A3** was treated with *endo*-norbornene dicarboxylic anhydride in the presence of NEt_3 to give monomer **M5** in 90% yield (Scheme 3). Monomer **M5** was subjected to ROMP but polymerization was not observed as indicated by the non-consumption of monomer by TLC, even after 38 h reaction. This demonstrated that *endo*-cis norbornene derivatives are not suitable candidates for ROMP using ruthenium catalysts as also supported by other reports [48–50].

The *exo*-norbornene-cored monomer **M3** was crystallized from

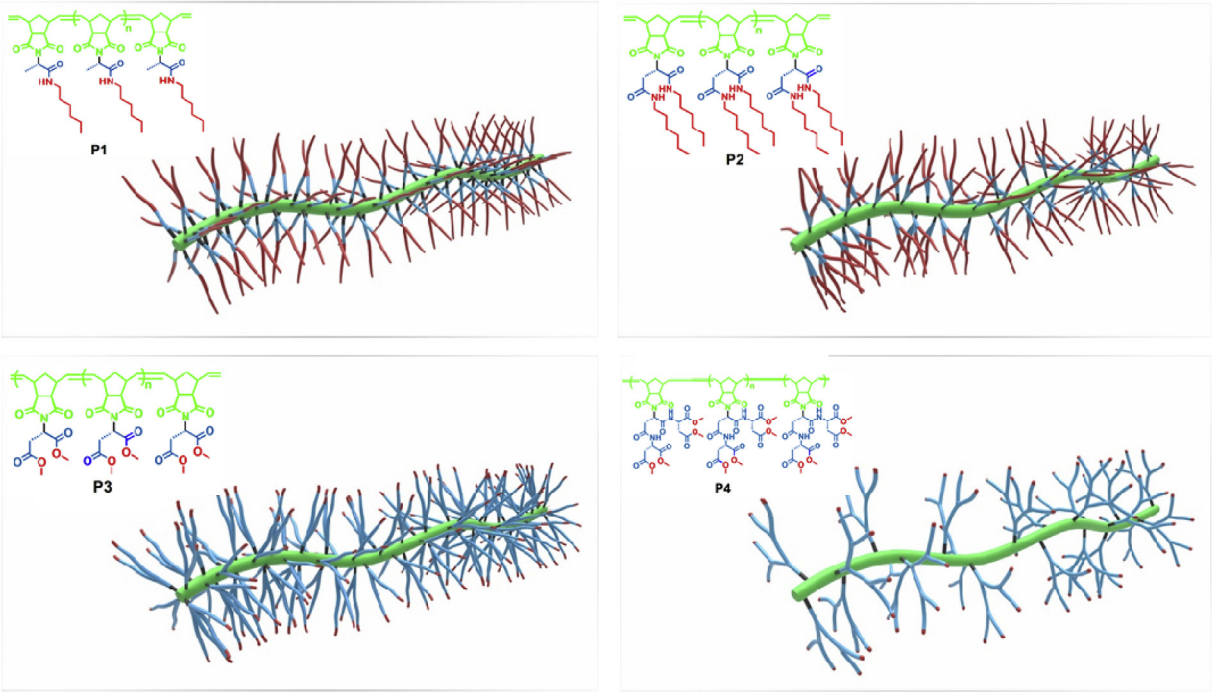

Fig. 3. Chemical structures of polymers **P1-P4** along with the graphical representation of bottlebrush polymeric architectures.

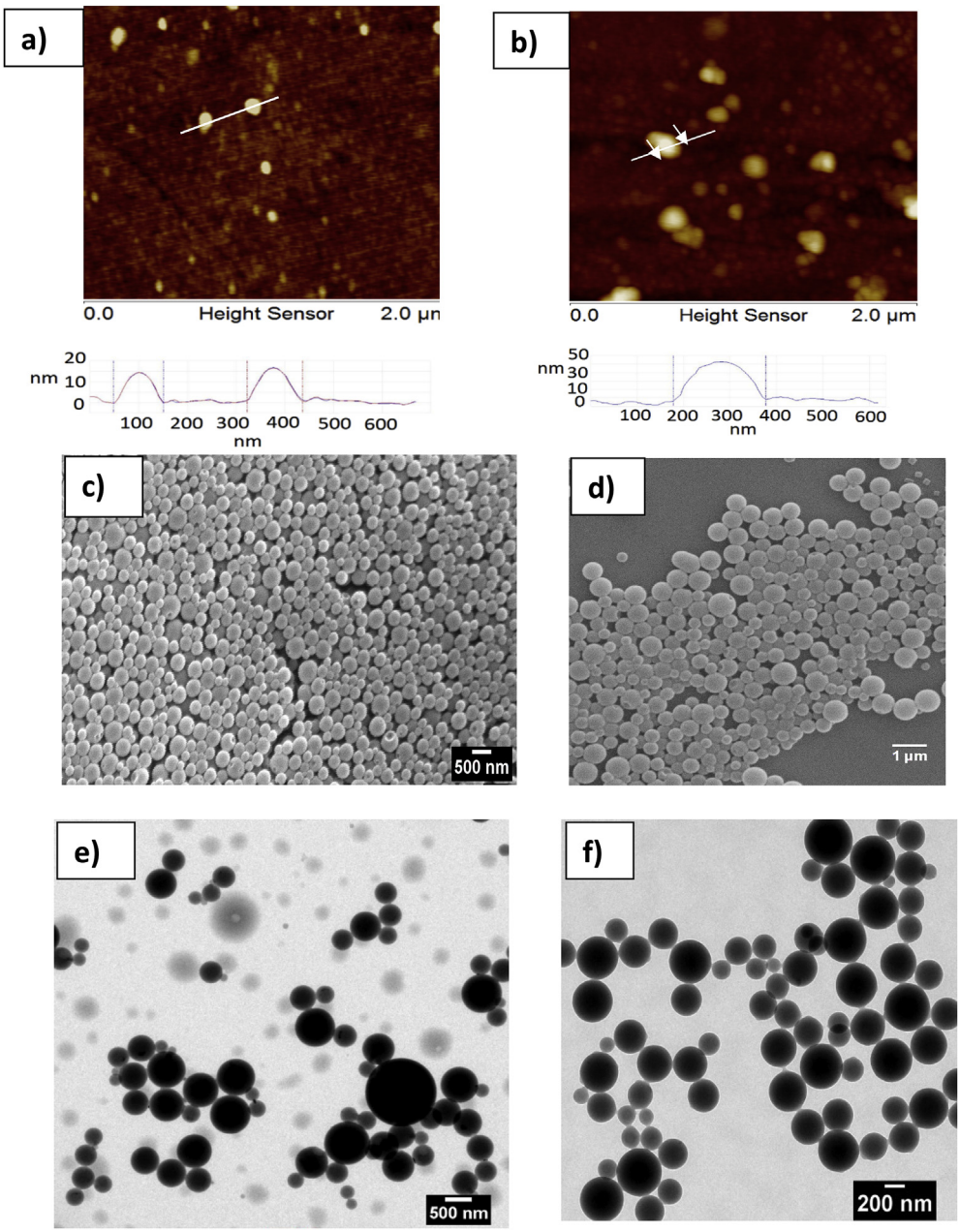

Fig. 4. AFM images in $CHCl_3$:MeOH (1:2) along with the cross sectional analysis of vesicles a) **P1**, b) **P3**; SEM image in $CHCl_3$:MeOH (1:2) c) **P1**, d) **P3**; TEM images in $CHCl_3$:MeOH (1:2) of e) **P1**, f) **P3.**

methanol. The single crystal X-ray structure of **M3** showed that the two sides of the norbornene skeleton (concave side and convex side) are easily accessible for the catalyst to trigger the polymerization (Fig. 7a-b and Table S1-S2).

The *endo*-geometry of **M5** showed no reactivity due to steric hindrance [50,56]. The other reason for the low reactivity of *endo*-isomer has been attributed to the catalyst inhibition due to the chelation of the propogating metallic center by *endo* functional group which prevents the coordination of the free monomer to the growing polymeric chain [48,50]. In the case of *exo*-isomer **M3**, this probability is ruled out as *exo*-imide functionality is too far to chelate with metallic center as evident from Fig. 7a-b. Hence, *exo*-isomers are more reactive towards ROMP as compared to *endo*-isomers.

4. Conclusions

We have successfully designed and synthesized a series of pseudopeptidic bottlebrush homopolymers based on *exo*-norbornene amino acids conjugates by using ring opening metathesis polymerization reaction. These polymers self-assembled to form the polymersomes of nanometer dimensions as characterized by various ultramicroscopic techniques. The comparison of self-assembling behavior of polymers demonstrated that the presence of higher number of lipid chains as well as branching in the polymeric framework do not affect the self-assembling properties. These polymersomes have good guest entrapment ability and therefore, has the potential for drug delivery application. In conclusion, we have demonstrated a simple designer strategy for the polymersomes from self-assembling peptide-based homopolymers.

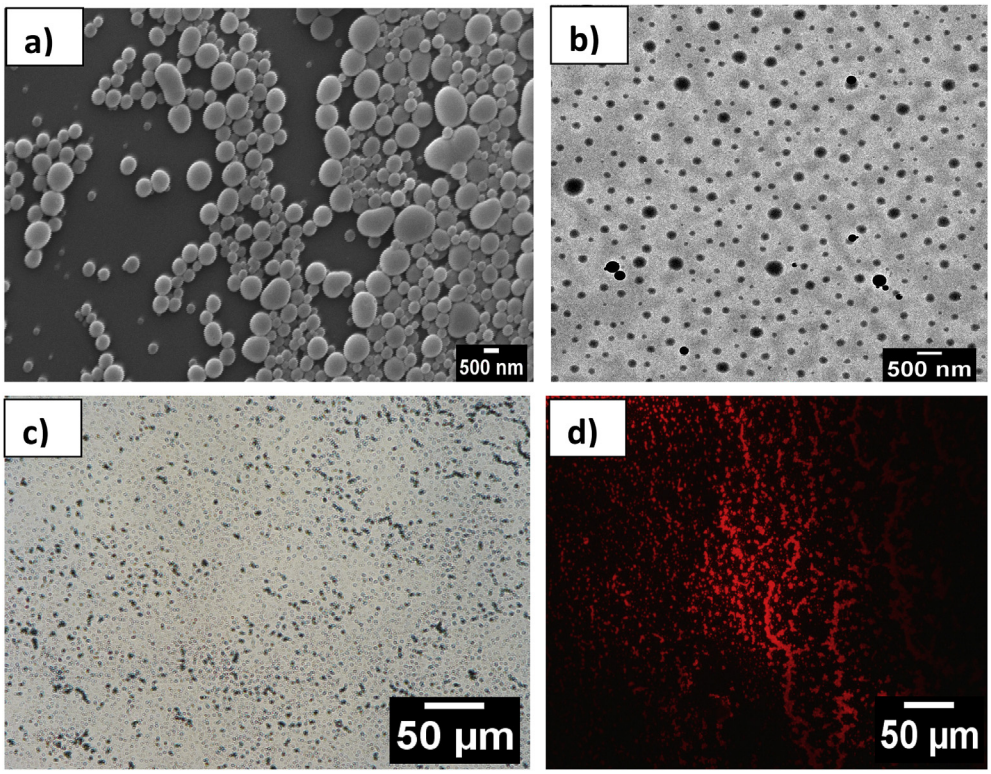

Fig. 5. Microscopic images of polymer **P2** a) SEM in 1:1 $CHCl_3$: MeOH, b) TEM in 1:1 $CHCl_3$: MeOH, c) Optical micrographs, d) Fluorescence microscopic image of **P2** + 0.02 equivalents of Rhodamine B in 1:1 $CHCl_3$: MeOH (λ_{ex} = 510-560 nm).

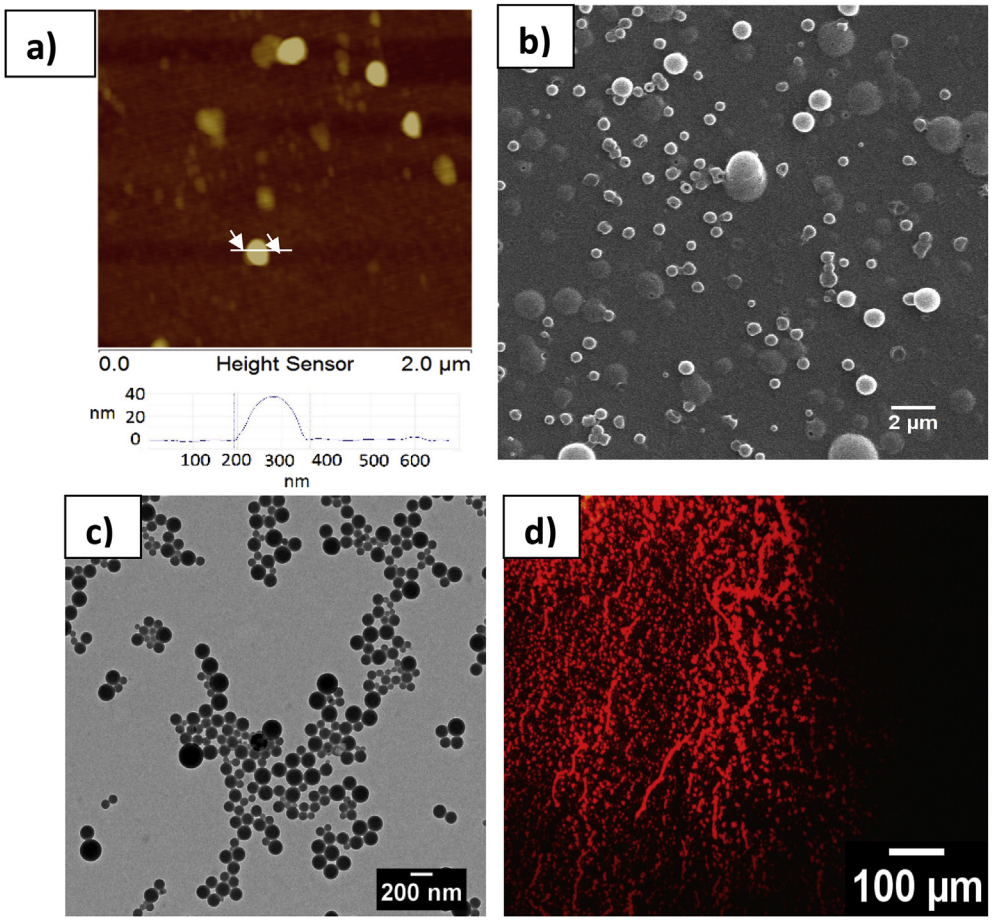

Fig. 6. Vesicular self-assembly of polymer **P4** a) AFM in 1:1 $CHCl_3$: MeOH along with the cross sectional analysis of vesicles, b) SEM in 1:1 $CHCl_3$: MeOH c) TEM in 1:1 $CHCl_3$: MeOH, d) Fluorescence microscopic image of **P4** + 0.02 equivalents of Rhodamine B in 1:1 $CHCl_3$: MeOH (λ_{ex} = 510-560 nm).

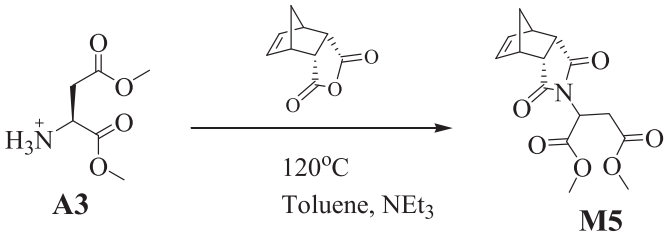

Scheme 3. Synthesis of *endo*-norbornene cored aspartic acid-based monomer **M5**.

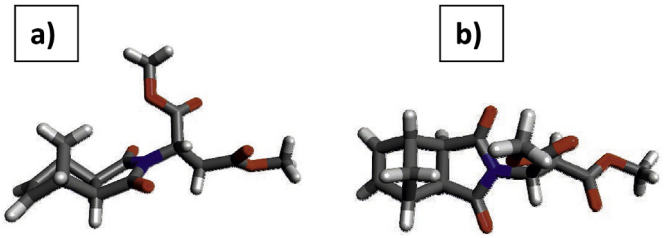

Fig. 7. X-ray crystal structure of **M3** (CCDC 1816299) a) side view b) top view.

Acknowledgements

We thank Department of Science and Technology DST, India for funding and FIST for mass spectral facility. SD thanks DST for the INSPIRE fellowship. BMB thanks UGC, India for the fellowship.

Appendix A. Supplementary data

Supplementary data related to this article can be found at https://doi.org/10.1016/j.polymer.2018.01.065.

References

[1] D.A. Tomalia, Dendrons/dendrimers: quantized, nano-element like building blocks for soft-soft and soft-hard nano-compound synthesis, Soft Matter 6 (3) (2010) 456–474, https://doi.org/10.1039/B917370F.
[2] J.S. Laursen, P. Harris, P. Fristrup, C.A. Olsen, Triangular prism-shaped β-peptoid helices as unique biomimetic scaffolds, Nat. Commun. 6 (2015) 7013, https://doi.org/10.1038/ncomms8013.
[3] D.J. Pochan, Z. Chen, H. Cui, K. Hales, K. Qi, K.L. Wooley, Toroidal Triblock copolymer assemblies, Science 306 (2004) 94–97, https://doi.org/10.1126/science.1102866.
[4] J. Sun, X. Chen, C. Deng, H. Yu, Z. Xie, X. Jing, Direct formation of giant vesicles from synthetic polypeptides, Langmuir 23 (2007) 8308–8315, https://doi.org/10.1021/la701038f.
[5] I.K. Kim, S.H. Kim, S.M. Choi, B.S. Youn, H.S. Kim, Extracellular vesicles as drug delivery vehicles for rheumatoid arthritis, Curr. Stem Cell Res. Ther. 11 (2016) 329–342.
[6] N.V.N. Jyothi, P.M. Prasanna, S.N. Sakarkar, K.S. Prabha, P.S. Ramaiah, G.Y. Srawan, Microencapsulation techniques, factors influencing encapsulation efficiency, J. Microencapsul. 27 (2010) 187–197, https://doi.org/10.3109/02652040903131301.
[7] S.B. Fonseca, M.P. Pereira, S.O. Kelley, Recent advances in the use of cell-penetrating peptides for medical and biological applications, Adv. Drug Deliv. Rev. 61 (2009) 953–964, https://doi.org/10.1016/j.addr.2009.06.001.
[8] A.D. Bangham, R.W. Horne, Negative staining of phospholipids and their structural modification by surface-active agents as observed in the electron microscope, J. Mol. Biol. 8 (1964) 660–668. https://doi.org/10.1016/S0022-2836(64)80115-7.
[9] J.M. Gebicki, M. Hicks, Ufasomes are stable particles surrounded by unsaturated fatty acid membranes, Nature 3243 (1973) 232.
[10] W.R. Hargreaves, D.W. Deamer, Liposomes from ionic, single-chain amphiphiles, Biochemistry (Mosc.) 17 (1978) 3759–3768, https://doi.org/10.1021/bi00611a014.
[11] A.R. Sapala, S. Dhawan, V. Haridas, Vesicles: self-assembly beyond biological lipids, RSC Adv. 7 (2017) 26608–26624, https://doi.org/10.1039/C7RA02746J.
[12] J. Du, R.K. O'Reilly, Advances and challenges in smart and functional polymer vesicles, Soft Matter 5 (2009) 3544–3561, https://doi.org/10.1039/b905635a.
[13] S. So, T.P. Lodge, Size control and fractionation of ionic liquid filled polymersomes with glassy and rubbery bilayer membranes, Langmuir 32 (2016) 4959–4968, https://doi.org/10.1021/acs.langmuir.6b00946.
[14] Y. Zhu, B. Yang, S. Chen, J. Du, Polymer vesicles: mechanism, preparation, application, and responsive behavior, Prog. Polym. Sci. 64 (2017) 1–22, https://doi.org/10.1016/j.progpolymsci.2015.05.001.
[15] B.M. Discher, Y.-Y. Won, D.S. Ege, J.C.-M. Lee, F.S. Bates, D.E. Discher, D.A. Hammer, Polymersomes: tough vesicles made from diblock copolymers, Science 284 (1999) 1143–1146, https://doi.org/10.1126/science.284.5417.1143.
[16] Y. Mai, A. Eisenberg, Self-assembly of block copolymers, Chem. Soc. Rev. 41 (2012) 5969–5985, https://doi.org/10.1039/c2cs35115c.
[17] R. Bleul, R. Thiermann, M. Maskos, Techniques to control polymersome size, Macromolecules 48 (2015) 7396–7409, https://doi.org/10.1021/acs.macromol.5b01500.
[18] D.E. Discher, A. Eisenberg, Polymer vesicles, Science 297 (2002) 967–973, https://doi.org/10.1126/science.1074972.
[19] T. Lammers, S. Aime, W.E. Hennink, G. Storm, F. Kiessling, TheranosticNanomedicine, Acc. Chem. Res. 44 (2011) 1029–1038, https://doi.org/10.1021/ar200019c.
[20] P.V. Pawar, S.V. Gohil, J.P. Jain, N. Kumar, Functionalized polymersomes for biomedical applications, Polym. Chem. 4 (2013) 3160–3176, https://doi.org/10.1039/c3py00023k.
[21] R.P. Brinkhuis, F.P.J.T. Rutjes, J.C.M. van Hest, Polymeric vesicles in biomedical applications, Polym. Chem. 2 (2011) 1449–1462, https://doi.org/10.1039/c1py00061f.
[22] H.-J. Choi, C.D. Montemagno, Artificial organelle: ATP synthesis from cellular mimetic polymersomes, Nano Lett. 5 (2005) 2538–2542, https://doi.org/10.1021/nl051896e.
[23] K.T. Kim, J.J.L.M. Cornelissen, R.J.M. Nolte, J.C.M. van Hest, A Polymersome Nanoreactor with controllable permeability induced by stimuli-responsive block copolymers, Adv. Mater. 21 (2009) 2787–2791, https://doi.org/10.1002/adma.200900300.
[24] S. Rameez, H. Alosta, A.F. Palmer, Biocompatible and biodegradable polymersome encapsulated hemoglobin: a potential oxygen carrier, Bioconjugate Chem. 19 (2008) 1025–1032, https://doi.org/10.1021/bc700465v.
[25] F. Ahmed, D.E. Discher, Self-porating polymersomes of PEG–PLA and PEG–PCL: hydrolysis-triggered controlled release vesicles, J. Contr. Release 96 (2004) 37–53, https://doi.org/10.1016/j.jconrel.2003.12.021.
[26] Y. Ohya, A. Takahashi, K. Nagahama, Biodegradable polymeric assemblies for biomedical materials, in: S. Kunugi, T. Yamaoka (Eds.), Polymers in Nanomedicine, vol 247, Springer Berlin Heidelberg, Berlin, Heidelberg, 2011, pp. 65–114.
[27] R. Gref, M. Lück, P. Quellec, M. Marchand, E. Dellacherie, S. Harnisch, T. Blunk, R.H. Müller, 'Stealth' corona-core nanoparticles surface modified by polyethylene glycol (PEG): influences of the corona (PEG chain length and surface density) and of the core composition on phagocytic uptake and plasma protein adsorption, Colloids Surfaces B Biointerfaces 18 (2000) 301–313, https://doi.org/10.1016/S0927-7765(99)00156-3.
[28] A. Carlsen, S. Lecommandoux, Self-assembly of polypeptide-based block copolymer amphiphiles, Curr. Opin. Colloid Interface Sci. 14 (2009) 329–339, https://doi.org/10.1016/j.cocis.2009.04.007.
[29] H. Iatrou, H. Frielinghaus, S. Hanski, N. Ferderigos, J. Ruokolainen, O. Ikkala, D. Richter, J. Mays, N. Hadjichristidis, Architecturally induced multiresponsive vesicles from well-defined polypeptides. Formation of gene vehicles, Biomacromolecules 8 (2007) 2173–2181, https://doi.org/10.1021/bm070360f.
[30] C. Sanson, C. Schatz, J.F. Le Meins, A. Soum, J. Thevenot, E. Garanger, et al., A simple method to achieve high doxorubicin loading in biodegradable polymersomes, J. Contr. Release 147 (2010) 428–435, https://doi.org/10.1016/j.jconrel.2010.07.123.
[31] F. Yamamoto, R. Yamahara, A. Makino, K. Kurihara, H. Tsukada, E. Hara, I. Hara, S. Kizaka-Kondoh, Y. Ohkubo, E. Ozeki, S. Kimura, Radiosynthesis and initial evaluation of ^{18}F labeled nanocarrier composed of poly(l-lactic acid)-block-poly(sarcosine) amphiphilic polydepsipeptide, Nucl. Med. Biol. 40 (2013) 387–394, https://doi.org/10.1016/j.nucmedbio.2012.12.008.
[32] D. Chow, M.L. Nunalee, D.W. Lim, A.J. Simnick, A. Chilkoti, Peptide-based biopolymers in biomedicine and biotechnology, Mater. Sci. Eng. R Rep. 62 (2008) 125–155, https://doi.org/10.1016/j.mser.2008.04.004.
[33] R.H. Grubbs, W. Tumas, Polymer synthesis and organotransition metal chemistry, Science 243 (1989) 907–915.
[34] R.R. Schrock, Living ring-opening metathesis polymerization catalyzed by well-characterized transition-metal alkylidene complexes, Acc. Chem. Res. 23 (1990) 158–165, https://doi.org/10.1021/ar00173a007.
[35] B.K. Keitz, A. Fedorov, R.H. Grubbs, Cis-selective ring-opening metathesis polymerization with ruthenium catalysts, J. Am. Chem. Soc. 134 (2012) 2040–2043, https://doi.org/10.1021/ja211676y.
[36] E.E. Yalçınkaya, O. Dayan, M. Balcan, Ç. Güler, Ring-opening metathesis polymerization of bicyclo[2.2.1]hepta-2,5-diene (norbornadiene) initiated by new ruthenium(II) complex, J. Appl. Polym. Sci. 127 (2013) 1691–1696, https://doi.org/10.1002/app.37867.
[37] G.M. Miyake, R.A. Weitekamp, V.A. Piunova, R.H. Grubbs, Synthesis of isocyanate-based brush block copolymers and their rapid self-assembly to infrared-reflecting photonic crystals, J. Am. Chem. Soc. 134 (2012) 14249–14254, https://doi.org/10.1021/ja306430k.
[38] K.D. Camm, N. Martinez Castro, Y. Liu, P. Czechura, J.L. Snelgrove, D.E. Fogg, Tandem ROMP–Hydrogenation with a third-generation Grubbs catalyst,

J. Am. Chem. Soc. 129 (2007) 4168–4169, https://doi.org/10.1021/ja071047o.
[39] S. Sutthasupa, F. Sanda, T. Masuda, ROMP of norbornene monomers carrying nonprotected amino groups with ruthenium catalyst, Macromolecules 42 (2009) 1519–1525, https://doi.org/10.1021/ma802243e.
[40] S. Sutthasupa, M. Shiotsuki, F. Sanda, Recent advances in ring-opening metathesis polymerization, and application to synthesis of functional materials, Polym. J. 42 (2010) 905–915, https://doi.org/10.1038/pj.2010.94.
[41] J. Hyvl, B. Autenrieth, R.R. Schrock, Proof of tacticity of stereoregular ROMP polymers through post polymerization modification, Macromolecules 48 (2015) 3148–3152, https://doi.org/10.1021/acs.macromol.5b00477.
[42] H.D. Maynard, S.Y. Okada, R.H. Grubbs, Synthesis of norbornenyl polymers with bioactive oligopeptides by ring-opening metathesis polymerization, Macromolecules 33 (2000) 6239–6248, https://doi.org/10.1021/ma000460c.
[43] H.D. Maynard, S.Y. Okada, R.H. Grubbs, Inhibition of cell adhesion to fibronectin by oligopeptide-substituted polynorbornenes, J. Am. Chem. Soc. 123 (2001) 1275–1279, https://doi.org/10.1021/ja003305m.
[44] M. Müllner, A.H.E. Müller, Cylindrical polymer brushes -anisotropic building blocks, unimolecular templates and particulate nanocarriers, Polymer 98 (2016) 389–401, https://doi.org/10.1016/j.polymer.2016.03.076.
[45] M. Zhang, C. Estournès, W. Bietsch, A.H.E. Müller, Superparamagnetic hybrid nanocylinders, Adv. Funct. Mater. 14 (2004) 871–882, https://doi.org/10.1002/adfm.200400064.
[46] M. Müllner, T. Lunkenbein, J. Breu, F. Caruso, A.H.E. Müller, Template-directed synthesis of silica nanowires and nanotubes from cylindrical core–shell polymer brushes, Chem. Mater. 24 (2012) 1802–1810, https://doi.org/10.1021/cm300312g.
[47] K. Huang, A. Jacobs, J. Rzayev, De novo synthesis and cellular uptake of organic nanocapsules with tunable surface chemistry, Biomacromolecules 12 (2011) 2327–2334, https://doi.org/10.1021/bm200394t.
[48] S. Kanaoka, R.H. Grubbs, Synthesis of block copolymers of silicon-containing norbornene derivatives via living ring-opening metathesis polymerization catalyzed by a ruthenium carbene complex, Macromolecules 28 (1995) 4707–4713, https://doi.org/10.1021/ma00117a050.
[49] S. Sutthasupa, K. Terada, F. Sanda, T. Masuda, Ring-opening metathesis polymerization of amino acid-functionalized norbornene derivatives, J. Polym. Sci. Part Polym. Chem. 44 (2006) 5337–5343, https://doi.org/10.1002/pola.21580.
[50] V. Lapinte, J.-C. Brosse, L. Fontaine, Synthesis and ring-opening metathesis polymerization(ROMP) reactivity of endo-and exo-norbornenylazlactone using ruthenium catalysts, Macromol. Chem. Phys. 205 (2004) 824–833, https://doi.org/10.1002/macp.200300120.
[51] L. Xiao, L. Qu, W. Zhu, Y. Wu, Z. Liu, K. Zhang, Donut-shaped nanoparticles templated by cyclic bottlebrush polymers, Macromolecules 50 (2017) 6762–6770, https://doi.org/10.1021/acs.macromol.7b01512.
[52] S.C. Radzinski, J.C. Foster, R.C. Chapleski, D. Troya, J.B. Matson, Bottlebrush polymer synthesis by ring-opening metathesis polymerization: the significance of the anchor group, J. Am. Chem. Soc. 138 (2016) 6998–7004, https://doi.org/10.1021/jacs.5b13317.
[53] L. Su, G.S. Heo, Y.-N. Lin, M. Dong, S. Zhang, Y. Chen, G. Sun, K.L. Wooley, Syntheses of triblock bottlebrush polymers through sequential ROMPs: expanding the functionalities of molecular brushes, J. Polym. Sci. Part Polym. Chem. 55 (2017) 2966–2970, https://doi.org/10.1002/pola.28647.
[54] K.J. Arrington, J.B. Matson, Assembly of a visible light photoreactor: an inexpensive tool for bottlebrush polymer synthesis *via* photoiniferter polymerization, Polym. Chem. 8 (2017) 7452–7456, https://doi.org/10.1039/C7PY01741C.
[55] M. Yang, W. Wang, F. Yuan, X. Zhang, J. Li, F. Liang, B. He, B. Minch, G. Wegner, Soft vesicles formed by diblock codendrimers of poly(benzyl ether) and poly(methallyl dichloride), J. Am. Chem. Soc. 127 (2005) 15107–15111, https://doi.org/10.1021/ja052713t.
[56] J.D. Rule, J.S. Moore, ROMP Reactivity of *endo*- and *exo* -Dicyclopentadiene, Macromolecules 35 (2002) 7878–7882, https://doi.org/10.1021/ma0209489.